Electrochemical and Solid-State Letters, **14** (11) H467-H469 (2011)
1099-0062/2011/14(11)/H467/3/$28.00 © The Electrochemical Society

Alleviating eSiGe Strain Relaxation Using Cryo-Implantation

C. L. Yang,[a,z] C. I. Li,[a] G. P. Lin,[a] I. M. Lai,[a] R. Liu,[a] H. Y. Wang,[a] B. C. Hsu,[a] M. Chan,[a] J. Y. Wu,[a] B. N. Guo,[b] B. Colombeau,[b] T. Wu,[b] and S. Lu[b]

[a]*United Microelectronics Corp., Central Research and Development Divison, Tainan 744, Taiwan*
[b]*Varian Semiconductor Equipment Associates, Inc., Gloucester, Massachusetts 01930, USA*

SiGe/Si hetero structure has been examined using high resolution x-ray diffraction for strain and cross sectional transmission electron microscopy for implant induced defects with various p-type source drain implant conditions at room or cryogenic temperature. The implant induced end-of-range defects can be reduced by optimizing Ge pre-amorphization implant energy and at cryogenic temperature. The alleviated strain relaxation and lower junction leakage current are correlated to the cryo-implant defect reduction.
 [DOI: 10.1149/2.023111esl]

Manuscript submitted June 14, 2011; revised manuscript received July 19, 2011. Published September 23, 2011.

For strained channel p-type metal-oxide-semiconductor (pMOS) devices, a uniaxial compressive stress in the channel is induced by the selective epitaxial growth (SEG) of embedded SiGe (eSiGe) in recessed source/drain (S/D) regions. Higher channel stress levels and lower SD resistance can be achieved by increasing the Ge content and the epilayer thickness in the S/D regions.[1] To be fully incorporated into Complimentary MOS (or CMOS) technology, these SiGe/Si layers will experience and have to withstand further processing steps, i.e. ion implantation and annealing. It is known that the subsequent spike rapid thermal process (sRTP) and Laser millisecond (msec) anneal could relax the strain by forming misfit and threading dislocations as lattices re-grown and dopants activated.[2,3] Ion implantation creates point defects, which act as nucleation sites for relaxation induced dislocation or aid in the inter-diffusion of Boron and Ge, resulting in accelerated strain relaxation.[4–6] This leads to a lower hole mobility and higher junction leakage therefore degrading device performance.

The evolution of end-of-range (EOR) defects and amorphization as a function of implant temperature have been reported previously.[7,8] The dynamic annealing process of interstitials and vacancies, generated by the implant, can be retarded by applying cryo temperature on substrate, resulting in deeper amorphization and smoother amorphous and crystal (a/c) interface layers. Cryo implants are well known to reduce Boron diffusion and activation anomalies.[7,9,10]

In this paper, eSiGe SD integrated in state-of-the-art 28 nm CMOS flow is studied for strain relaxation. The strain is characterized with high resolution x-ray diffraction (HRXRD) rocking curves. The defects are examined with cross sectional transmission electron microscopy (XTEM) and correlated to the junction leakage. The modulation of injected silicon interstitial on the strain relaxation processes at the SiGe/Si interface after 1015°C sRTP and 1250°C Laser msec annealing, coupled with cryo temperature pMOS source and drain (PSD) implants, are investigated. The cryo-implants were conducted at −100°C. The junction leakage related to the defect propagated from SiGe layer to Si substrate after msec anneal are discussed.

The recessed SiGe S/D junction was fabricated and integrated with 28 nm device flow.[11] SiGe on Si substrate was epitaxial-grown (EPI) by low pressure chemical vapor deposition. The p/n junction was formed by in-situ doped SiGe EPI and followed with PSD implants. The PSD implant conditions include same Boron implant along with different Ge energies (10, 12, or 15 keV) with the same dosage of 5e14 atoms/cm^2 and combination of either of cryo or room temperature (RT). sRTP and msec anneals were applied to recover the implant damage and to activate the dopants. The strain relaxation and implant damage were characterized by HRXRD and XTEM.

[z] E-mail: Chan_Lon_Yang@umc.com

Fig. 1 shows the HRXRD rocking curves collected after eSiGe EPI deposition, PSD (Ge 15 keV RT and Boron RT) implants, sRTP, and Laser msec anneal, respectively. The high intensity peak is silicon peak and the relaxed SiGe is to the left as labeled in Fig. 1. The strain level is determined by the peak position. The greater the distance between the Si and relaxed SiGe peaks, the higher the strain in the Si capping layer. The full-width-half-maximum (FWHM) of rocking curve peaks is inversely related to the thickness of film layers and defects within the layers. A fringe pattern is clearly seen around the SiGe peak for the as-grown strained SiGe EPI layer. This indicates almost no misfit dislocation generated at the SiGe/Si interface and maintained its original strain and crystallinity. After implant, the rocking curve showed relaxed SiGe peaks shifted to the left with decreased peak intensity. This implies the shift in lattice constant and some strain relaxation potentially induced by Ge implant. After sRTP and msec anneal, SiGe peak broadened, peak position shifted to the right, and peak intensity decreased. This indicates that most of the strain relaxations were resulted from the re-crystallization after sRTP and msec anneal steps. The implant induced defects act as dislocation sources and aggregate SiGe strain relaxation shown as the SiGe peak broadening. The shift in SiGe peak positions reflects the Ge/Boron diffusion post thermal annealing. The broadening Si peak with much larger FWHM after msec anneal reflects the defects existed in the Si substrate.

The SiGe/Si interface quality and the strain relaxation are determined from the extent of defects after sRTP and msec anneal steps. The EOR defects, formed around a/c interface, are the main contributor for strain relaxation. Post SiGe amorphization implant with different Ge energies (10, 12, or 15 keV) with the same dosage (Fig. 1b) can modulate the amount of interstitials released from the EOR defects toward the SiGe/Si interface and introduce varying degree of strain relaxation from different damaged SiGe layer after re-crystallization anneal. From HR-XRD shown in Fig. 1b, with 10 keV Ge cryo-implant, both fringe pattern and strain relaxation are recovered and similar to the as deposited results. The amount of strain relaxation can be extracted from HRXRD rocking curves from the software and procedures described in.[12] The strain relaxation can be improved from RT 28% (Fig. 1a) to close to no relaxation for 10 keV Ge cryo-implant (Fig. 1b). There could be two mechanisms for such observed energy effects even all at cryo-temperature: 1) the deeper EOR for 15 keV Ge implant is closer to SiGe/Si interface and defects could be propagated deeper around the SeGe/Si interface, or 2) the shallower EOR for 10 keV Ge implant is closer to the wafer surface and these defects could be resolved faster.[13]

The micro-structures of the SiGe EPI layer integrated with implant, sRTP, and msec anneal steps, are revealed in XTEM images shown in Fig. 2. Two types of defects, misfit dislocation from the SiGe/Si interface and 60° threading dislocation inside the SiGe as well as defects in the Si substrate can be observed for the Ge 15 keV RT implant XTEM (Fig. 2a). The SiGe/Si interface with reduced defects (60° threading dislocation) can still be observed for the Ge 15 keV cryo-implants in Fig. 2b. The defect free from cryo implant for Ge

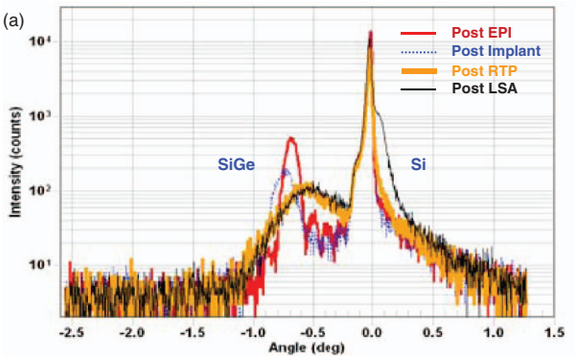

Figure 1. (a) HRXRD rocking curves for eSiGe/Si strain relaxation collected after SiGe EPI deposition, SD implant (Ge 15 keV, 5e14 atoms/cm^2), sRTP, and msec anneal, respectively. (b) HRXRD rocking curves for Ge energy response (10, 12, and 15 keV) after anneal (sRTP/msec) coupled with cryo temperature (−100°C).

10 keV split (Fig. 2c) is in agreement with no Si peak broadening as shown in HRXRD rocking curves (Fig. 1a).

The improvements for the strain relaxation and defect reduction from the Ge energy optimization and cryo-implant also demonstrated from the junction leakage for different PSD implant conditions (Fig. 3). The leakage for Ge 15 kV cryo-implant has narrower distribution than Ge 15 keV RT implant. Ge 10 keV implant at cryo temperature results in the leakage current reduction by ∼2 orders than Ge 15 keV at RT which consists with less defects and defect free in Si substrate as shown in Fig. 1 TEM's respectively. In case of eSiGe SD junction, the leakage current generated in the silicon substrate increases with the lattice misfit defects, junction profile changes from dopant distribution, and from the band gap reduction.[14] Since the Ge concentration is kept the same in this study (implanted Ge concentration are insignificant relative to the in-situ incorporated Ge), there is no difference from the band gap reduction. As reported in,[11]

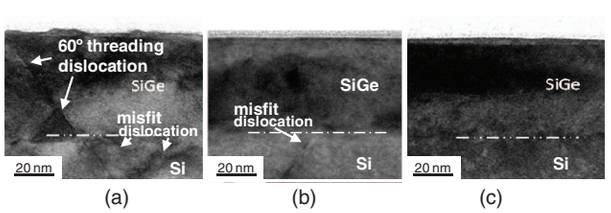

Figure 2. XTEM after spike/msec anneal for PSD implants at (a) Ge 15 keV at RT, (b) Ge 15 keV at cryo temperature, (c) Ge 10 keV at cryo temperature (−100°C).

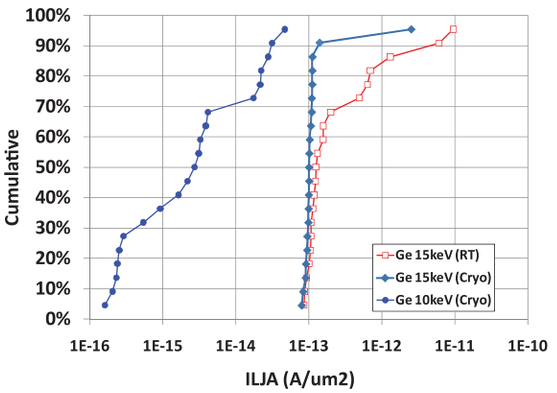

Figure 3. Junction leakage comparison for RT and cryo implants for Ge at either 15 or 10 keV. Ge 10 keV cryo-implants showed ∼2 orders leakage mean value reduction relative to Ge 15 keV RT implant conditions.

the cryo-implant results in ∼6 nm shallower junction compared to RT implant. Therefore higher leakage current would be expected for cryo-implant due to the higher doping density induced higher electric field and higher trap-assisted tunneling factor. The lower leakage from cryo implant shown in Fig. 3 can be explained using defect related mechanism. Relaxation of the misfit strain can generate misfit dislocation and threading dislocation which may propagate into the depletion region in the silicon substrate, and thus increase the leakage current by reducing the generation lifetime as explained in.[14]

In summary, the strain relaxation from PSD implants for SiGe/Si layers formed with full 28 nm CMOS integration flow was investigated. The strain relaxation with RT implants is observed in HRXRD rocking curves. The high misfit dislocation defects in SiGe film and EOR dislocation in silicon substrate are revealed from the XTEM images. Post SiGe amorphization implant with different Ge energies modulates the amount of interstitials released from the EOR defects. This introduces varying degree of strain relaxation from different damaged SiGe layer toward the SiGe/Si interface after re-crystallization sRTP anneal. The following msec anneal enhances the propagation and formation of the dislocation defects. With the EOR defects reduction, using optimized Ge implant energy coupled with cryo temperature, the strain relaxation can be significantly alleviated as shown in the fringe patterns of HRXRD rocking curves. The lower junction leakage confirms the physical characterizations.

References

1. L. Washington, F. Nouri, S. Thirupapuliyur, G. Eneman, P. Verheyen, V. Moroz, L. Smith, X. Xu, M. Kawaguchi, T. Huang, K. Ahmed, M. Balseanu, L.-Q. Xia, M. Shen, Y. Kim, R. Rooyackers, K. De Meyer, and R. Schreutelkamp, *IEEE Electron Device Lett.*, **27**, 511 (2006).
2. O. Fujii, T. Sanuki, Y. Oshiki, T. Itani, T. Kugimiya, N. Nakamura, M. Tamura, T. Sato, I. Mizushima, H. Yoshimura, M. Iwai, and F. Matsuoka, *VLSI Tech.*, pp 156, (2009).
3. M. H. Yu, J. H. Li, H. H. Lin, C. H. Chen, K. C. Ku, C. F. Nieh, H. Hisa, Y. M. Sheu,C. W. Tsai, Y. L. Wang, H. Y. Chu, H. C. Cheng, T. L. Lee, S. C. Chen, M. S. Liang, *IEDM Tech. Dig.* (2006).
4. J. P. Liu, A. Domenicucci, A. Madan, J. Li, J. Holt, and John Sudijono, *Appl. Phys. Lett.* **88**, 151916 (2006).
5. Y. Hoshi, K. Sawano, A. Yamada, N. Usami, K. Arimoto, K. Nakagawa, and Y. Shiraki, *Journal of App. Phys.* **107**, 103509, (2010).
6. R. T. Crosby, K. S. Jones, M. E. Law, A. F. Saavedra, J. L. Hansen, A. N. Larsen, and J. Liu, *Mat. Res. Soc. Symp. Proc.* **810**, C4.12, (2004).
7. F. Khaja, B. Colombeau, T. Thanigaivelan, D. Ramappa, and T. Henry, *Int. Conf. Ion Implantation Technology Proc.*, pp. 65–68, (2010).
8. A. Jain, J. J. Chambers, and J. B. Shaw, *Int. Conf. Ion Implantation Technology Proc.*, 31–36 (2010).
9. J. A. Van den Berg, D. G. Armour, S. Zhang, S. Whelan, H. Ohno, T.-S. Wang, A. G. Cullis, E. H. J. Collart, R. D. Goldberg, P. Bailey and T. C. Q. Noakes, *J. Vac. Sci. Technol.* **B20**(3) 974–983, (2002).
10. K. Suguro, A. Murakoshi, T. Iinuma, H. Akutsu, T. Shibata, Y. Sugihara, K. Okumura, *Mater. Res. Soc. Proc.* 669 (2001).

11. C. I. Li, C. L. Yang, H. Y. Hsieh, G. P. Lin, R. Liu, H. Y. Wang, B. C. Hsu, M. Chan, J. Y. Wu, I. C. Chen, B. N. Guo, B. Colombeau, K. H. Shim, T. Wu, H. L. Sun, and S. Lu, *Int. Workshop on Junction Technology Proceedings*, 71–74, (2011).
12. http://www.jordanvalley.com/
13. B. Colombeau, A. J. Smith, N. E. B. Cowern, B. J. Pawlak, F. Cristiano, R. Duffy, A. Claverie, C. J. Ortiz, P. Pichler, E. Lampin, C. Zechner, *Mat. Res. Soc. Symp. Proc.* Vol. 810, C3.6.1–12, (2004).
14. E. R. Simoen, G. Eneman, P. Verheyen, R. Loo, M. B. Gonzalez, and C. Claeys, *ECS Transactions*, **16**(10) 513–527, (2008).